International Atomic Energy Agency

INDC(CPR)-013/LI
INT(88)-1

INDC INTERNATIONAL NUCLEAR DATA COMMITTEE

PRELIMINARY ANALYSIS OF NEUTRON OPTICAL POTENTIAL FOR A = 40-60 BELOW 10 MeV

Zongdi SU*
Nuclear Physics Laboratory,
Oxford University,
Oxford, United Kingdom

December 1988

* Permanent Address: Institute of Atomic Energy, Beijing, China

IAEA NUCLEAR DATA SECTION, WAGRAMERSTRASSE 5, A-1400 VIENNA

INDC(CPR)-013/LI

PRELIMINARY ANALYSIS OF NEUTRON OPTICAL POTENTIAL FOR A = 40-60 BELOW 10 MeV

Zongdi SU*
Nuclear Physics Laboratory,
Oxford University,
Oxford, United Kingdom

December 1988

* Permanent Address: Institute of Atomic Energy, Beijing, China

Reproduced by the IAEA in Austria
December 1988

88-05789

PRELIMINARY ANALYSIS OF NEUTRON OPTICAL POTENTIAL FOR $A = 40 \sim 60$ BELOW 10 MEV†

Su Zong Di*
Nuclear Physics Laboratory, Oxford, U.K.

Abstract

The variation of the total cross section σ_t and the absorption cross section σ_a with the parameters of the spherical optical potential (SOP) at low neutron energies for the nuclei in the region of the maximum strength function ($A = 40 \sim 60$) has been studied. These results show that the dependence of σ_t and σ_a on the parameters of the SOP and neutron energy is very complicated. For the dependence of the cross section on the SOP, the real potential parameters are more sensitive than the imaginary potential ones, and the real potential depth V_0 and real radius parameter r_R are the most sensitive parameters in the SOP. The behaviours of the total cross section with varying SOP parameters depend strongly on the neutron energy and are very different for the different nuclei. The results has shown why the existing parametrizations do not give a good agreement with experimental data for low neutron energies in this mass region. The processes and results shown in this paper are significant to obtain the best parametrization for fitting the experimental data.

1. Introduction

The optical model provides the basis for many theoretical analyses that are used in reproducing experimental data and supplying nuclear data for application. In addition to offering a convenient means for the calculations of the neutron total cross section, shape elastic cross section and angular distribution, optical potentials are widely used in DWBA analyses and, most importantly, in supplying transmission coefficients for Hauser-Feshbach statistical theory calculations. The most important tasks in all these applications of the optical model is to determine the optical model parameters. One of the long-standing task here is the search for a unique set of optical potential parameters which can accuratly describe as much experimental data as possible in wide regions of neutron energies and nuclear masses. In recent years some important analyses of the existing parametrizations have been made by P.G.Young[1)] (1985), V.A.Konshin

†This work is supported by the International Atomic Energy Agency.

* Permanent address: Institute of Atomic Energy, Beijing, People's Republic of China.

and O.V.Konshin[2] (1987) respectively. Thirteen kinds of global spherical optical parametrizations[3−15] available, from the first parametrization[3] to the latest ones[11,15] have been included in their analysis. The comparative analyses of the different parametrizations of the spherical optical potential (SOP) have shown that parametrizations of SOP which fit the higher energies experimental data very accurately tend to give total cross sections that can not reproduce the experimental data at low energies for the nuclei in the region of the maximum strength function ($A = 40 \sim 60$). From Fig.1 which is taken from Ref.[1] one can see that in the total cross sections for ^{40}Ca no existing parametrization discribes a deep minimum in σ_t for neutron energies below 4 MeV. At higher energies a satisfactory agreement with experimental data can be reached by using parameters [3], [10] and [11]. The same problem at low energies also takes place ^{58}Ni and here the critical energy is below 3 MeV. For higher energies a good agreement with experimental data for ^{58}Ni can be obtained by using parameters [4], [10] and [11]. The fact that the level excitation functions can not be reproduced by any existing parametrizations in the mass region above A=40 is also quite serious.

We want to discuss this problem from other approach. The variation of the total cross section σ_t and the absorption cross section σ_a with the parameters of the SOP for different neutron energies has been studied. These results show that the dependence of σ_t and σ_a on the parameters of the SOP and neutron energy is very complicated. We have shown why the existing parametrizations [3~15] do not give a good agreement with experimental data for low neutron energies in this mass region. The processes and results shown in this paper are significant to obtain the best parametrization for fitting the experimental data.

2. The parameters of the SOP

A standard representation of the phenomenological SOP is used thoughout the paper:

$$U(r,E) = -V_R(E)f_R(r) - iW_V(E)f_V(r) + i4a_D W_D(E)\frac{d}{dr}f_D(r)$$
$$+\left(\frac{\hbar}{m_\pi c}\right)^2 \frac{V_{SO}}{r}(\mathbf{l}\cdot\boldsymbol{\sigma})\frac{d}{dr}f_{SO}(r) \qquad (1)$$

where

$$f_i(r) = [1+\exp(\tfrac{r-R_i}{a_i})]^{-1} \qquad i = R, V, D, SO$$
$$R_i = r_i A^{1/3} \qquad i = R, V, D, SO$$

and

$$
\begin{array}{lll}
V_R(E) = V_0 - 0.31E & (\text{MeV}) & \\
W_V(E) = 0 & (\text{MeV}) & \\
W_D(E) = W_0 + 0.4E & (\text{MeV}) & (2) \\
V_{SO} = 6 & (\text{MeV}) & \\
r_{SO} = 1.2 & (\text{fm}) & \\
a_{SO} = 0.5 & (\text{fm}) &
\end{array}
$$

The fact that $W_V(E) = 0$ is due to analysed neutron energy region $E_N \leq 10$ MeV in this analysis, and the attention focusses mainly on parameters V_0, r_R, a_R, W_0, r_D, and a_D. The analytical process is as follows : We study respectively the variation of σ_t and σ_a with various optical model parameter for the different neutron energies, whilst fixing the other ones in their reasonable regions. The optical model paramerters of reference are as follows :

$$
\begin{array}{lll}
V_0 = 48.54 & (\text{MeV}) & \\
r_R = 1.27 & (\text{fm}) & \\
a_R = 0.68 & (\text{fm}) & (3) \\
W_0 = -2.4 & (\text{MeV}) & \\
r_D = 1.27 & (\text{fm}) & \\
a_D = 0.58 & (\text{fm}) &
\end{array}
$$

3. The results and analyses

The total cross section and absorption cross section for the interaction of neutrons with ^{40}Ca and ^{58}Ni are calculated at neutron energies E_N =0.5, 0.7, 1.0, 1.5, 2.0, 3.0, 4.0, 5.0, 7.0 and 10.0 MeV. The resulting values of the total cross section and the absorption cross section are shown as a function of the constant term V_0 of the real potential depth at the above energies for ^{40}Ca and ^{58}Ni, shown in Figs. 2 $\sim$ 5. As well as the absorption cross section, σ_a/σ_t is also very important in learning about the fraction occupied by the absorption in the total cross section for the Hauser-Feshbach theory calculation in Figs. 3 and 5. The difference between Fig. 4(a) and Fig. 4(b) is only that different radius parameter of the real potential are used. The latter being $r_R = 1.21$ fm. The differece between Fig. 4(a) and Fig. 4(c) is only that different surface diffuseness of the real potential are used. The latter being $a_R = 0.62$ fm. The comparisons of the various results show that the variational characteristic of the curves seems similar, but they are displaced.

The other sensitive parameter of the SOP is the real radius parameter r_R. The calculated results of σ_t, σ_a and σ_a/σ_t as a function of r_R are presented in Figs.6 $\sim$ 9. The results of Fig. 8(a), (b) and (c) are obtained with the different parameter V_0 which are taken as 46.54 MeV, 48.54 MeV and 50.54 MeV respectively. The comparisons of these results show that the variational characteristic seems similar, but they are displaced.

The above results show that the variances of the cross section and absorption cross section with increasing real potential depths and radii are quite complicated. The variational behaviour of the total cross section with increasing V_0 and r_R is very different for the different energies. The results of Fig. 10 and Fig. 11 show the changing character of the total cross section with varying V_0 and r_R within a wider range of the parameter variation. The fluctuations of the total cross section are especially violent for energies less than about 5 MeV. For lower energies, the total cross section can change by $\sim$ 25% on increasing r_R by 1 %. The variation of the total cross sections with increasing V_0 and r_R is very large for the lower energies.

The calculated results of σ_t, σ_a and σ_a/σ_t as a function of a_R are presented in Figs. 12 $\sim$ 15. These results show that the variation of the cross section with increasing real surface diffuseness do not fluctuate so greatly as those with V_0 and r_R. The total cross section can change by $\sim$ 7 % (the greatest) when increasing a_R by 10 % at E_N=3.0 MeV for ^{40}Ca, and it can change by 9 % (the greatest) at E_N=0.5 MeV for ^{58}Ni when increasing a_R by increasing a_R by 10 %. In addition, even though the neutron energy is the same, the behaviours of the total cross sections with increasing a_R are very different for the various nuclei.

The calculated results of σ_t, σ_a and σ_a/σ_t as a function of W_0 are presented in Figs. 16 $\sim$ 19. The comparison between Fig. 16 and Fig. 18 show that the behaviours of the total cross section for ^{40}Ca and ^{58}Ni are different. For several lower energies, as W_0 is raised the total cross sections for ^{40}Ca increase, but the situation for ^{58}Ni proves to be the contrary. The greatest variances of the total cross section can change by 5 % when increasing W_0 by 10 %.

The calculated results of σ_t, σ_a and σ_a/σ_t as a function of r_D and a_D are presented in Figs. 20 $\sim$ 23 and Figs. 24 $\sim$ 27 respectively. These results show that the variations of the cross sections are very small and W_0, r_D and a_D raised σ_a and σ_a/σ_t increase very slowly. The greatest change in the total cross section is $\sim$ 6 % on increasing r_D or a_D by 10 %.

4. Conclusions

The calculations made to study the sensitivity of optical model results on variations of the potential parameters for the interaction of neutrons with nuclei ^{40}Ca and ^{58}Ni show that :

a). For the dependence of the cross section on the SOP, the real potential parameters are more sensitive than the imaginary potential ones, and the real potential depth V_0 and real radius parameter r_R are the most sensitive parameters in the SOP. Small changes in V_0 or r_R lead to great variations in the cross section. The total cross section can change by $\sim$25 % on increasing V_0 or r_R by 1 %, and by $<$ 1 % on increasing the other parameters by 1 %.

b). The results clearly show that the behaviours of the total cross section with varying SOP parameters depend strongly on the neutron energy. The variations of the total cross section with varyng the SOP parameters are the more extreme, the lower neutron energy. For energies below about 1 MeV, the total cross sections with increasing V_0 or r_R fluctuate quite violently. However, for the higher neutron energies, the variations of total cross section with increasing the SOP parameters are smaller.

The results also show that the variations of the cross section with increasing the SOP parameters are very different for different energies. The total cross sections increase with some SOP parameter for some energies, decrease for some energies,and fluctuate or do not change for other energies.

c). For a given neutron energy, the behaviours of the cross sections with varying SOP parameter are very different in the same range of the optical potential parameter for the different nuclei. For exampe, we can compare the results of Fig. 2 and Fig. 4 or Fig. 6 and Fig. 8. The total cross sections decrease with increasing V_0 or r_R for ^{40}Ca, but increase for ^{58}Ni below about 1 MeV. The total cross sections increase with increasing V_0 or r_R for ^{40}Ca, but decrease for ^{58}Ni when neutron energies are 3, 4 and 5 MeV. As might be expected, the total cross sections increase with increasing V_0 or r_R for energies above 5 MeV in the parameter ranges of Fig. 2 and Fig. 4 or Fig. 6 and Fig. 8. For different nuclei the dependence of the total cross sections on the SOP parameters is so different that it is very difficult to get a unique set of the optical potential parameters which can accurately describe as much experimental data as possible in a wide regions of neutron energies and nuclear masses.

d). We can not look for a set of the optical potential parameter to accord with the experimental data for the above ten energies simultaneously, regardless of whether we are ^{40}Ca or ^{58}Ni in all these Figs. of the total cross section–the SOP parameter. Therefore it is not strange for us that no parametrizition as mentioned above can reproduce the experimental data of lower energies and higher energies at the same time.

Many authors have discussed this problem using different approaches to resolve this difficulty. Finlay *et al*[16] (1985) proposed to introduce the energy dependent geometry parameter – a new and important step. One might get the impression that at low energies a behaviour of the optical potential changes and the necessily arises for the introduction of the non-traditional energy dependence of potential parameters. It is, of course, possible to accommodate these and other departures from the simple optical model by more complicated parametrisations, but in the absence of theoretical guidance concerning the form of parametrisations, these are inevitably arbitrary and are unlikely to be applicable outside the domain where they are fitted to experimental data.

The other method, a consistent analysis for the neutron total cross sections using dispersion relations that connect the real and imaginary part of optical potential at low energies was provided [17]. The contribution of the surface component in dispersion relations has the effect of increasing the effective radius and the surface diffuseness of the real potential. As previously pointed out, the behaviours of the total cross sections with increasing radius are different for the different neutron energies. Therefor, it is difficult too to improve in agreement with experimental data for all energies.

e). The results show too that the σ_a and σ_a/σ_t with increasing W_0, r_D and a_D increase slowly.

These results show that the total neutron cross sections at low energies is governed by an interference effects [18] that make it rather sensitive to quite small changes of some parameters in the SOP. This is presumable due to a Ramsauer-like interference effect, between the waves going through the nucleus and those going around it.

I would like to thank Dr. P.E. Hodgson and M.B. Chadwick for helpful discussions.

References

[1] Young P.G., Proc. of the Specialists' Meeting on the Use of the Optical Model for the Calculation of Neutron Cross Sections Below 20 MeV, Paris, 1985, P. 125.

[2] Konshin V.A. and Konshin O.V., The IAEA Advisory Group Meeting on Nuclear Theory for Fast Neutron Data Evalution, Beijing, 12-16 October 1987.

[3] Moldauer P.A., *Nucl. Phys.*, **47**(1963)65.

[4] Wilmore D. and Hodgson P.E., *Nucl. Phys.*, **55** (1964)673.

[5] Perey F.G. and Buck B., *Nucl. Phys.*, **32**(1962)353.

[6] Engelbrecht C.A. and Fiedeldey H., *Ann. Phys.*, **42**(1967)262.

[7] Becchetti F.D. and Greenlees G.W., *Phys. Rev.*, **182**(1969)1190.

[8] Patterson D.G. *et al.*, *Nucl. Phys.*, **A263**(1976)261.

[9] Madland D.C. and Young P.G., Proc. of the Intern. Conf. on Neutron Physics and Nuclear Data for reactors and Other Applications, Harwell, OECD, 1978, P.349.

[10] Rapaport J. *et al.*, *Nucl. Phys.*, **A330**(1979)15.

[11] Walter R.L. and Guss P., Proc. of the Intern. Conf. on NUclear Data for Basic and Applied Science, Santa Fe, 1985.

[12] Fu C.Y. and Hetrick D.M., *Update of ENDF/B-V Mod.-3 Iron, Producing Cross Sections and Energy-Angle Correlation*, ORNL/TM-9964, 1964.

[13] Pasechnik M.V. *et al.*, Proc. of the Conf. on Neutron Physics, Kiev, 1972, part 1, P.253.

[14] Bersillon O. *et al.*, Proc. of the Intern. Conf. on Nuclear Data for Science and Techn, Antwerp, 1982, P.665.

[15] Kikuchi I. and Sekine N., *Evaluation of Neutron Nuclear Data of Natural Nickel and its Isotopes for JENDL-2*, JAERI-M85-101, 1985, P.195.

[16] Finlay R.W. *et al.*, *Phys.Let.*, **155B**(1985)313.

[17] Su Zong Di and Hodgson P.E., (To be published).

[18] Bowen P.H.*et al.*, *Nucl.Phys.*, **22**(1961)640.

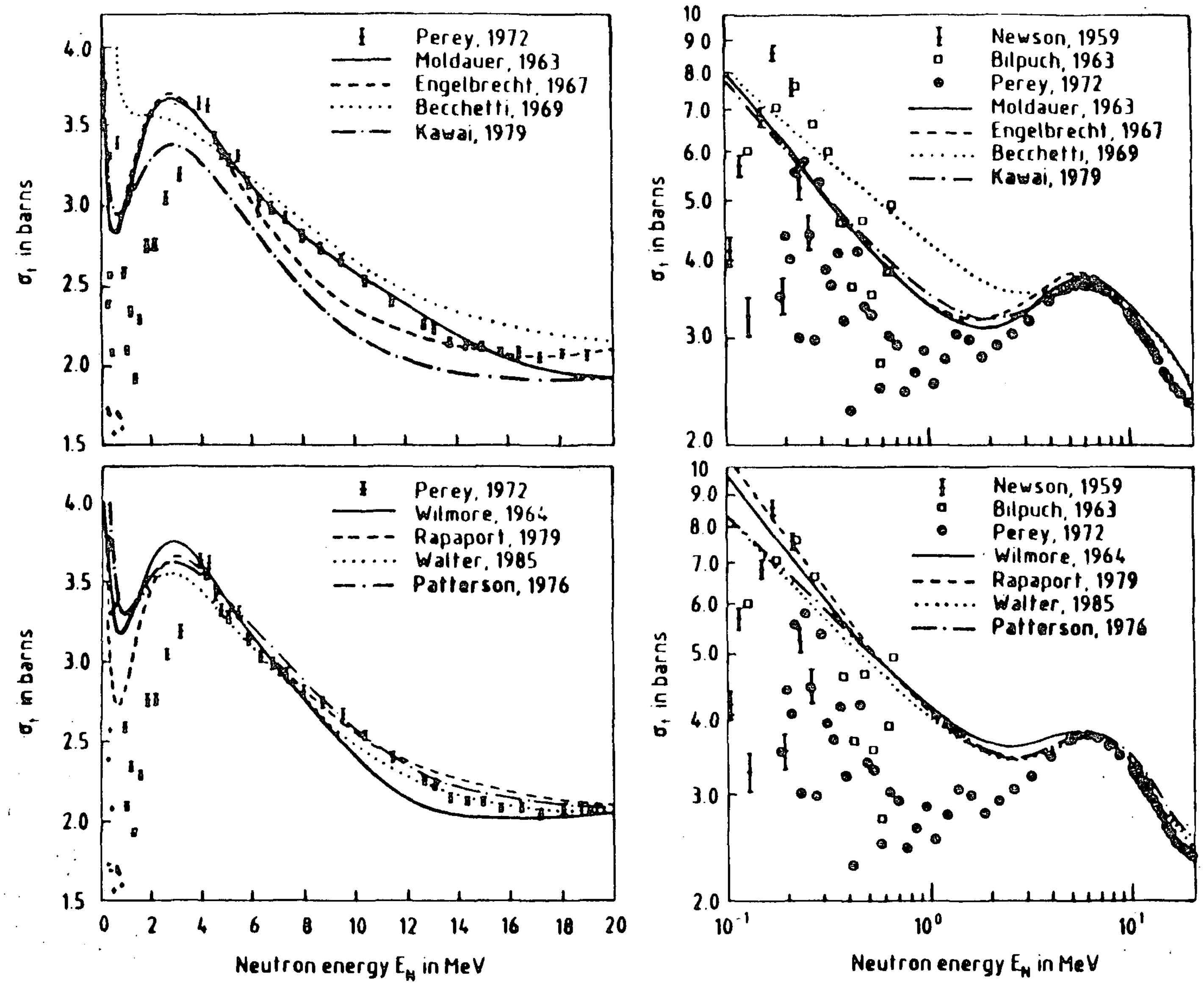

(a) Total cross-sections for neutrons on ^{40}Ca (b) Total cross-sections for neutrons on ^{58}Ni

Fig.1 Comparison of experimental and calculated total cross section data for the interaction of neutrons with ^{40}Ca and ^{58}Ni. The figure is taken from [1].

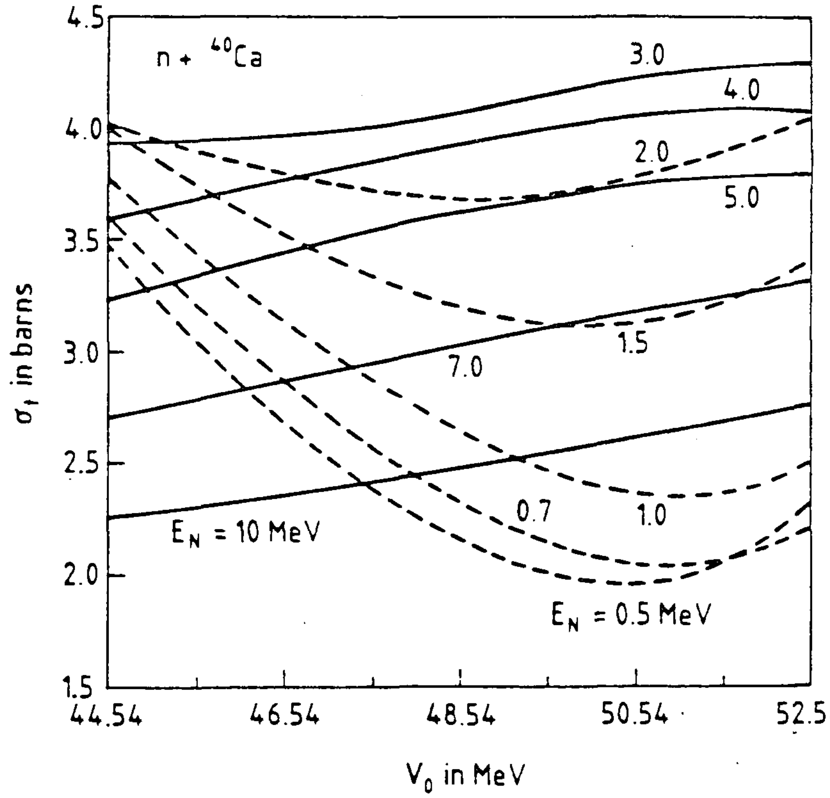

Fig.2 Total cross section for the interaction of neutrons with ^{40}Ca as a function of the constant term V_0 of the real potential depth for several energies. It is notable that the total cross sections increase with V_0 roughly in use full curves, but decrease in using dashed curves (the same for the below Figs.).

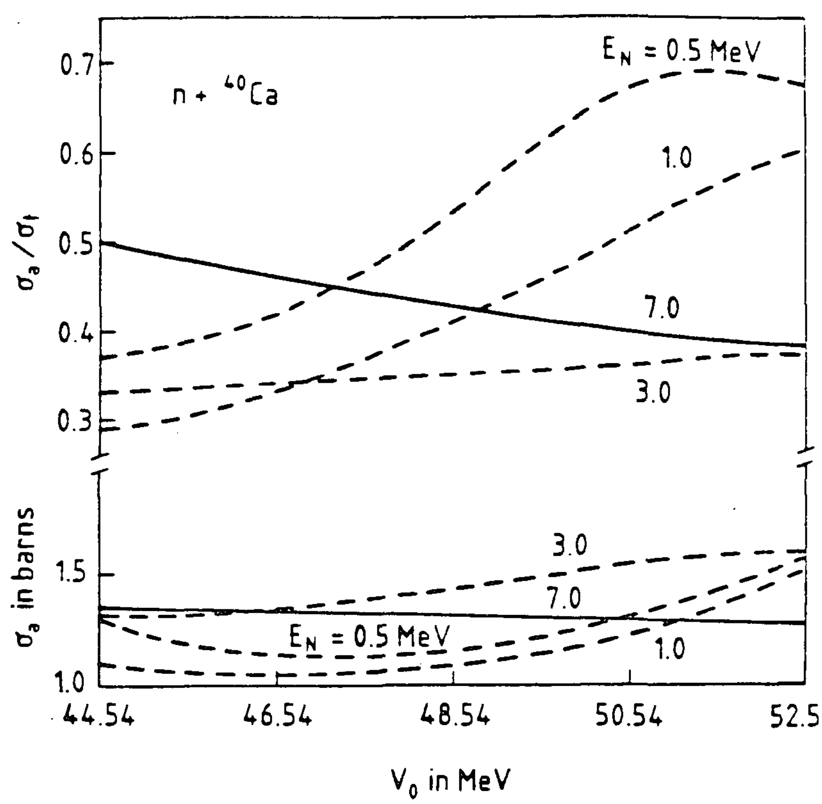

Fig.3 Absorption cross section and σ_a/σ_t for the interaction of neutrons with ^{40}Ca as a function of the constant term V_0 of the real potential depth for several energies. It is notable that the total cross sections increase with V_0 roughly in use full curves, but decrease in use dashed curves (the same for the below Figs.).

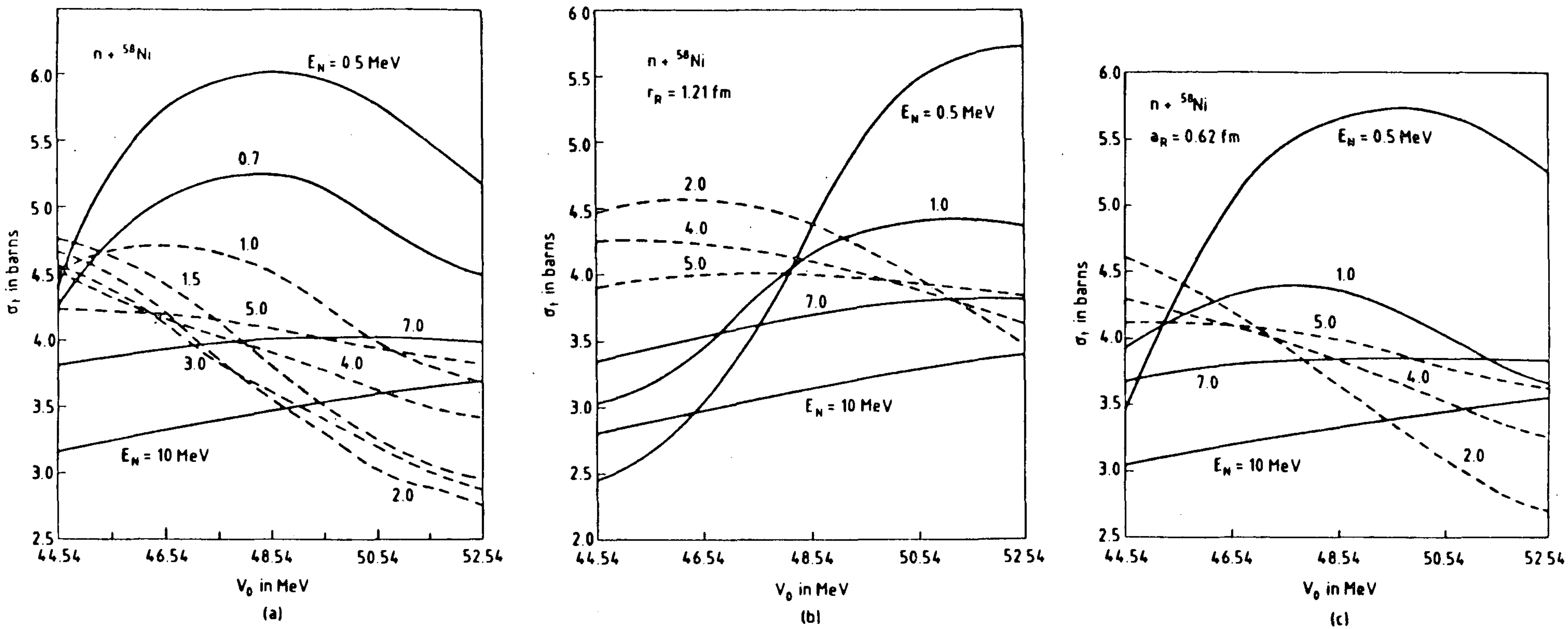

Fig.4 Total cross section for the interaction of neutrons with ^{58}Ni as a function of the constant term V_0 of the real potential depth for several energies. The parameters are taken from formulae (1) $\sim$ (3) in Fig. (a). We take r_R=1.21 fm in Fig. (b) and a_R=0.62 fm in Fig. (c) respectively.

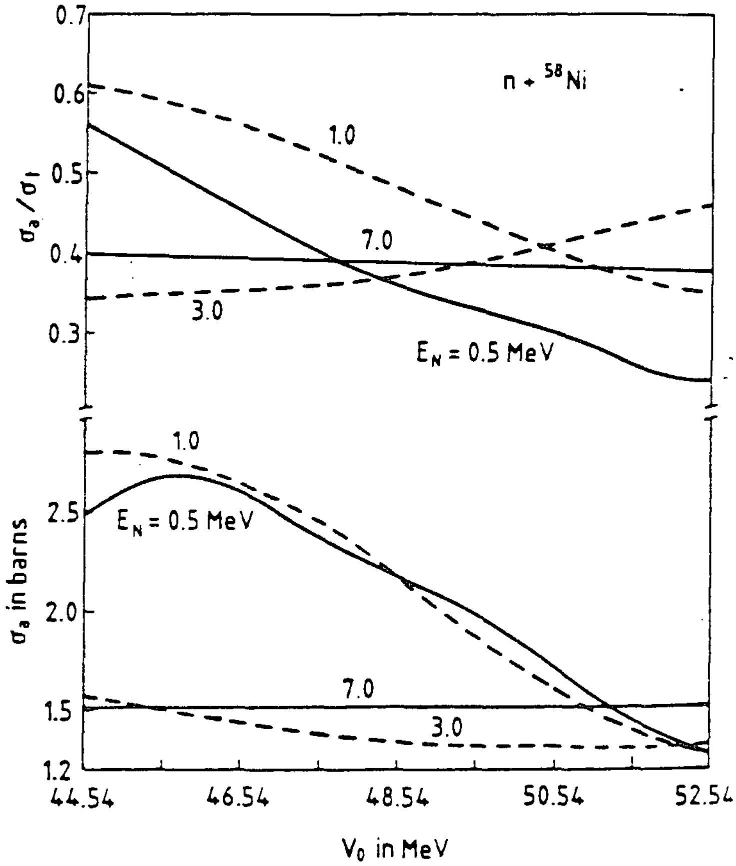

Fig.5 Absorption cross section and σ_a/σ_t for the interaction of neutrons with ^{58}Ni as a function of the constant term V_0 of the real potential depth for several energies.

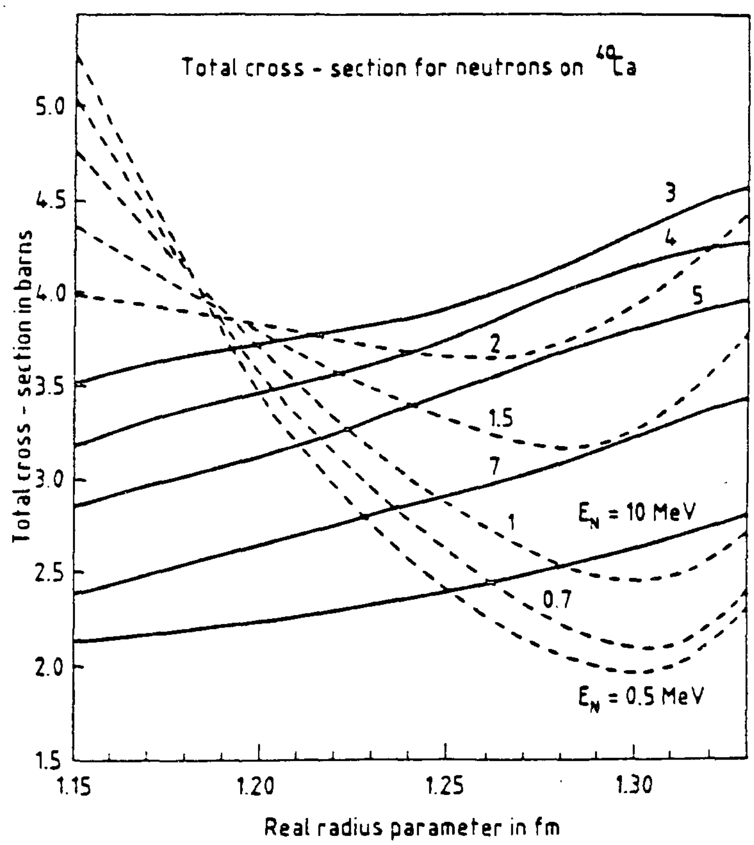

Fig.6 Total cross section for the interaction of neutrons with ^{40}Ca as a function of the radius parameter r_R of the real potential for several energies.

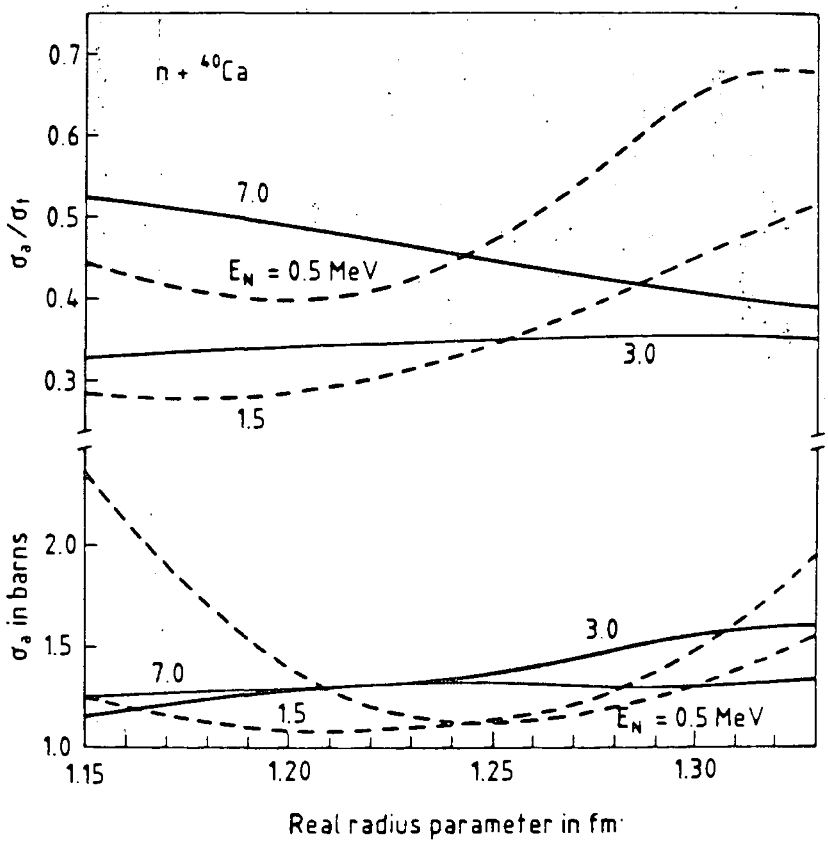

Fig.7 Absorption cross section and σ_a/σ_t for the interaction of neutrons with ^{40}Ca as a function of the radius parameter r_R of the real potential for several energies.

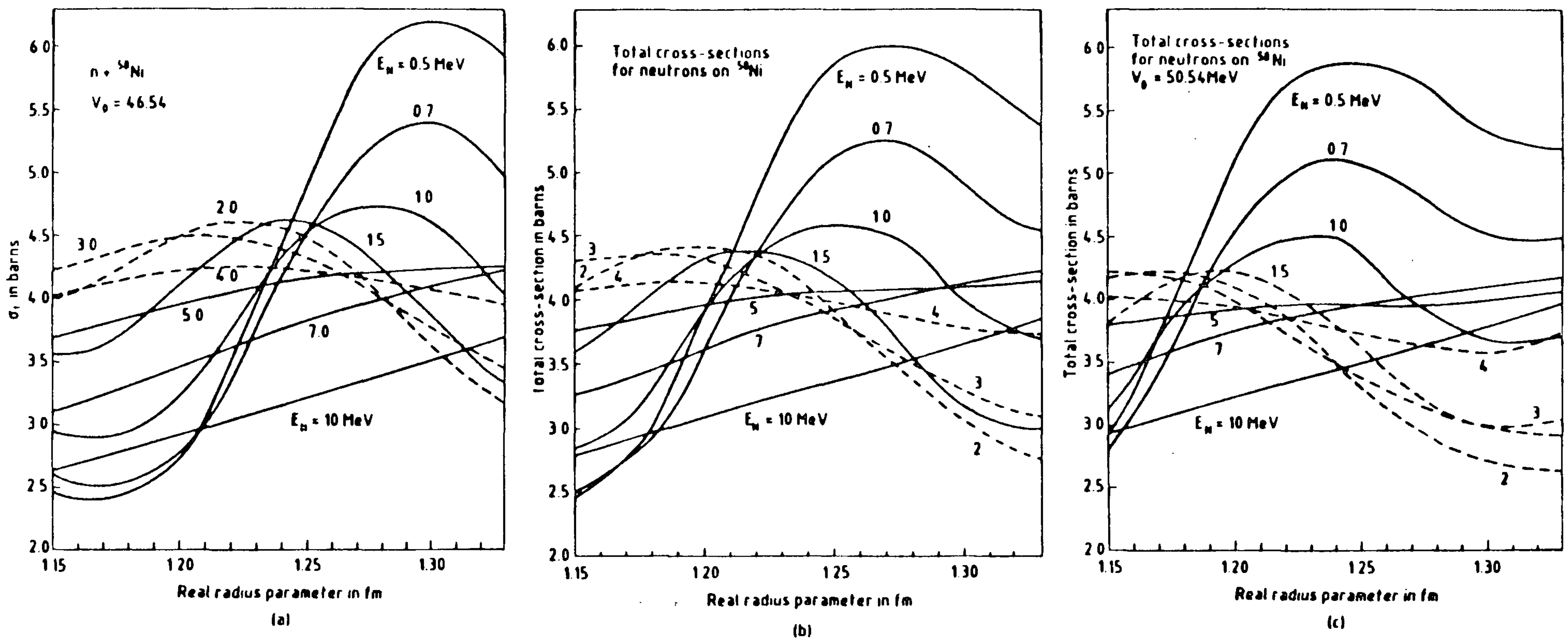

Fig.8 Total cross section for the interaction of neutrons with ^{58}Ni as a function of the radius parameter r_R of the real potential for several energies, where (a) V_0=46.54 MeV; (b) V_0=48.54 MeV; (c) V_0=50.54 MeV.

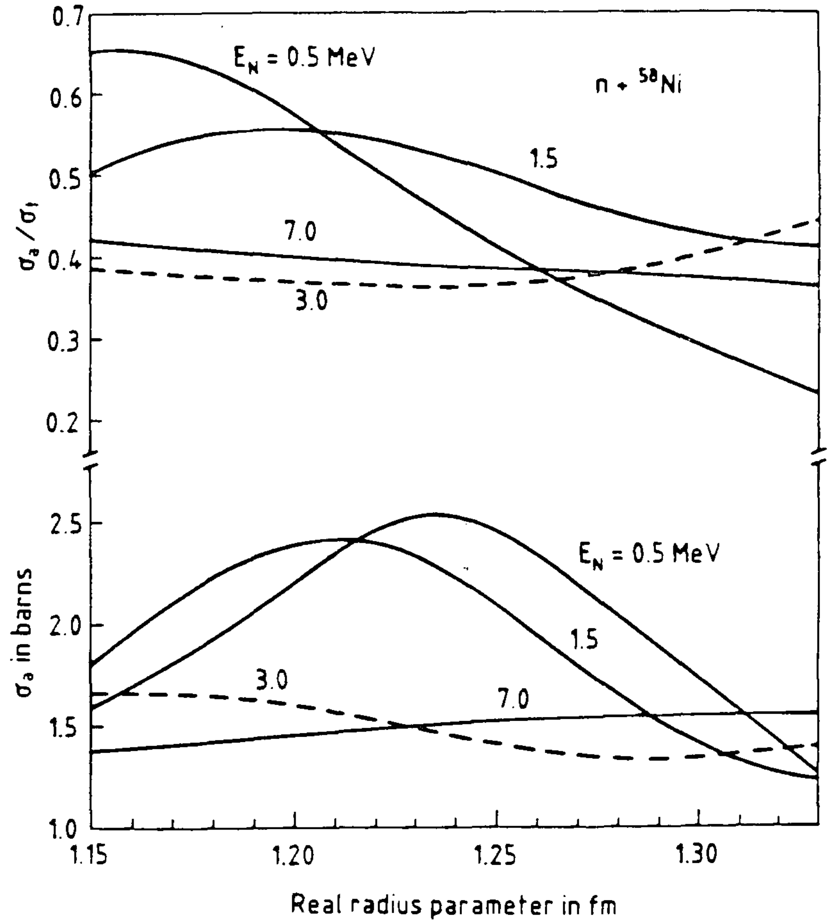

Fig.9 Absorption cross section and σ_a/σ_t for the interaction of neutrons with ^{58}Ni as a function of the radius parameter r_R of the real potential for several energies.

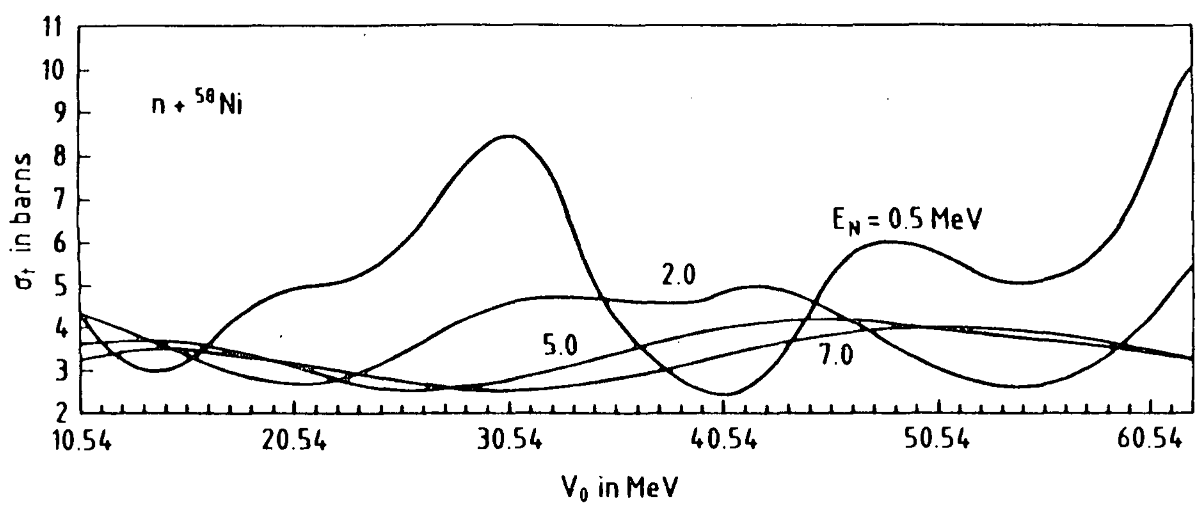

Fig.10 Variational behaviour of total cross section for the interaction of neutrons with ^{58}Ni with varying V_0 within a wider range for several energies selected E_N=0.5, 2.0, 5.0 and 7.0 MeV.

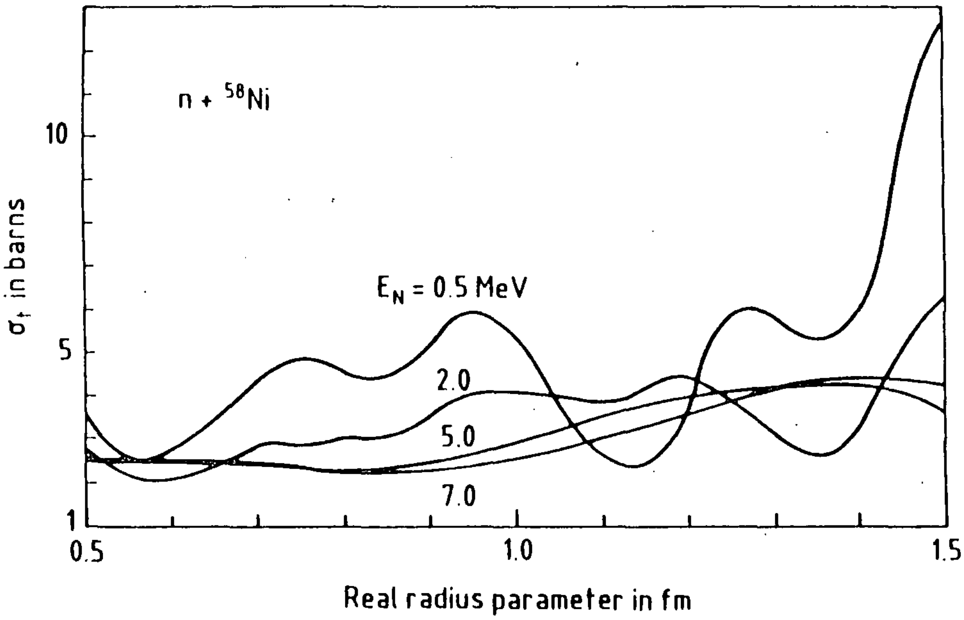

Fig.11 Variational behaviour of total cross section for the interaction of neutrons with ^{58}Ni with varying r_R within a wider range for several energies selected E_N=0.5, 2.0, 5.0 and 7.0 MeV.

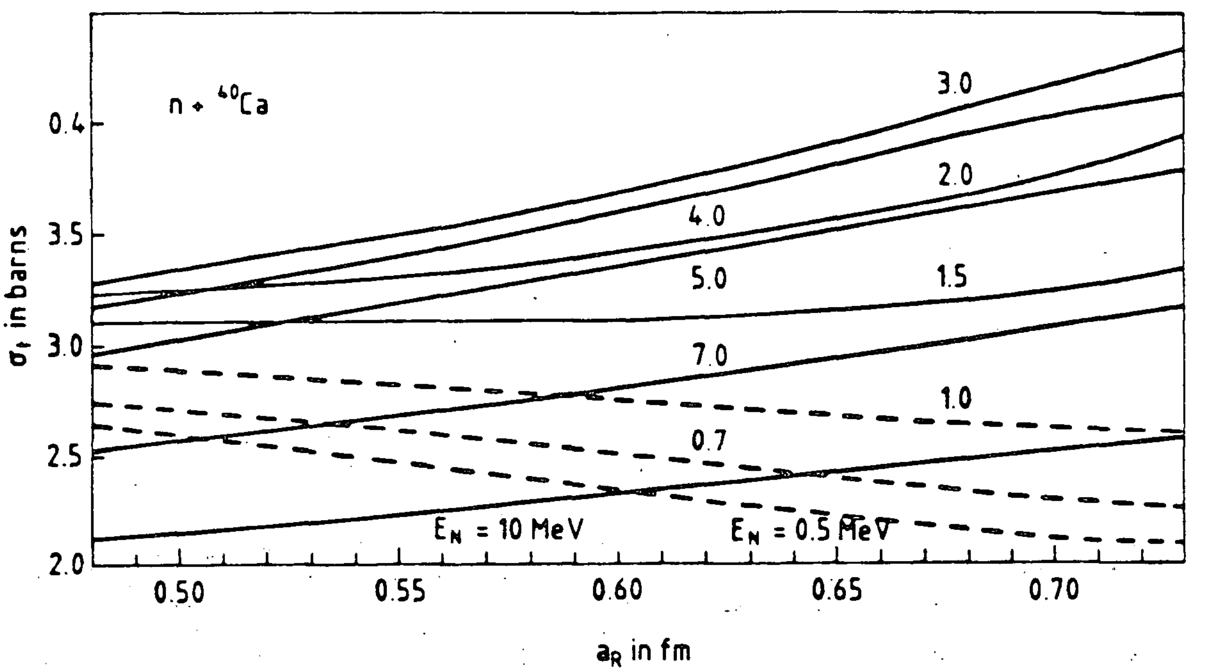

Fig.12 Total cross section for the interaction of neutrons with ^{40}Ca as a function of the surface diffuseness parameter a_R of the real potential for several energies.

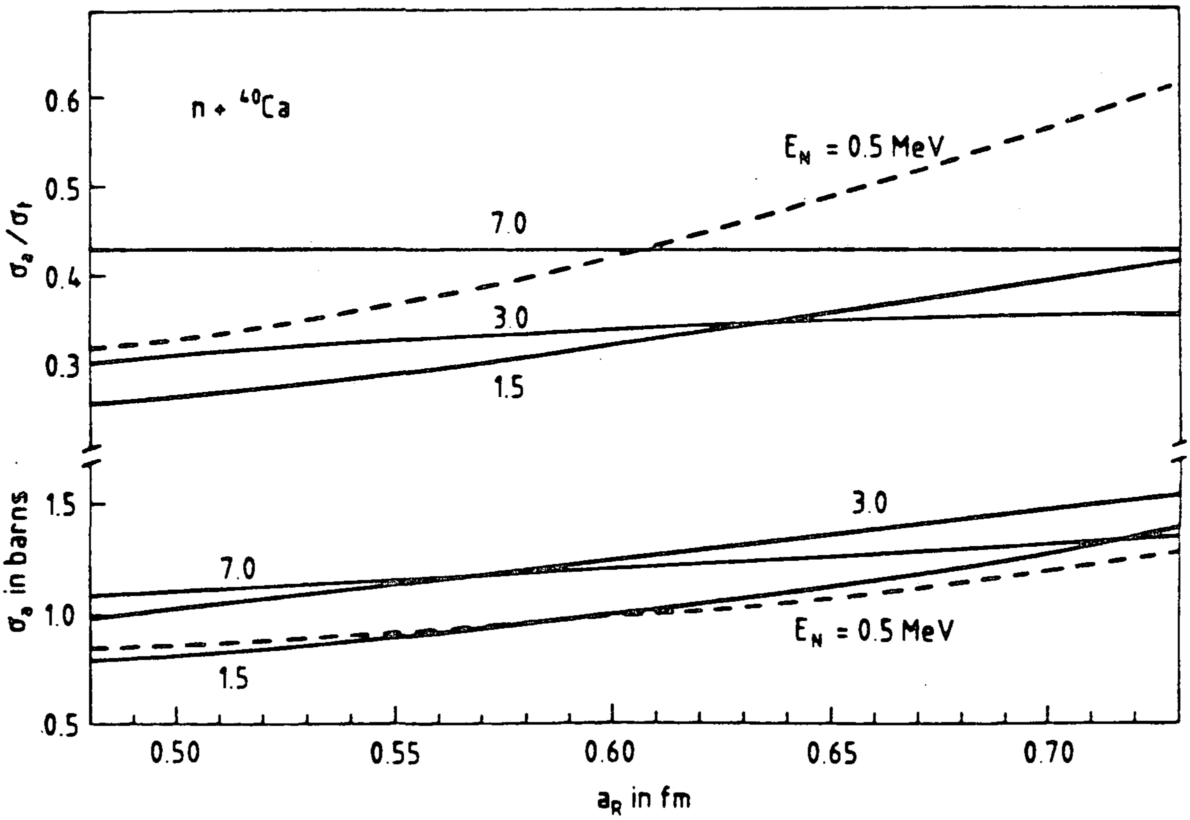

Fig.13 Absorption cross section and σ_a/σ_t for the interaction of neutrons with ^{40}Ca as a function of the surface diffuseness parameter a_R of the real potential for several energies.

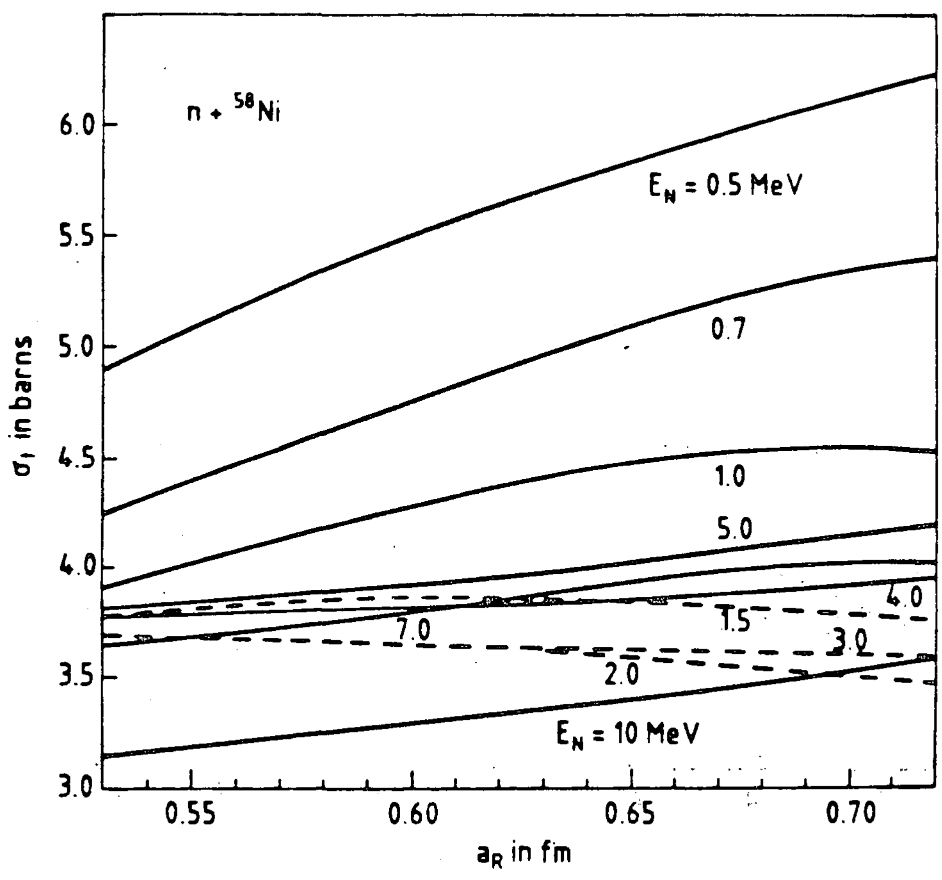

Fig.14 Total cross section for the interaction of neutrons with ^{58}Ni as a function of the surface diffuseness parameter a_R of the real potential for several energies.

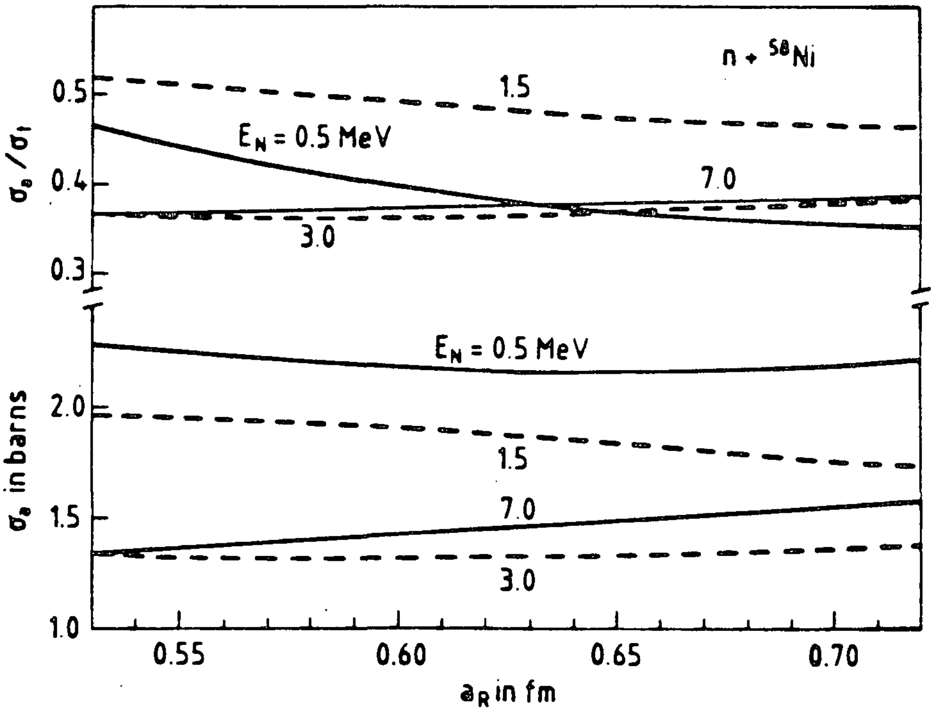

Fig.15 Absorption cross section and σ_a/σ_t for the interaction of neutrons with ^{58}Ni as a function of the surface diffuseness parameter a_R of the real potential for several energies.

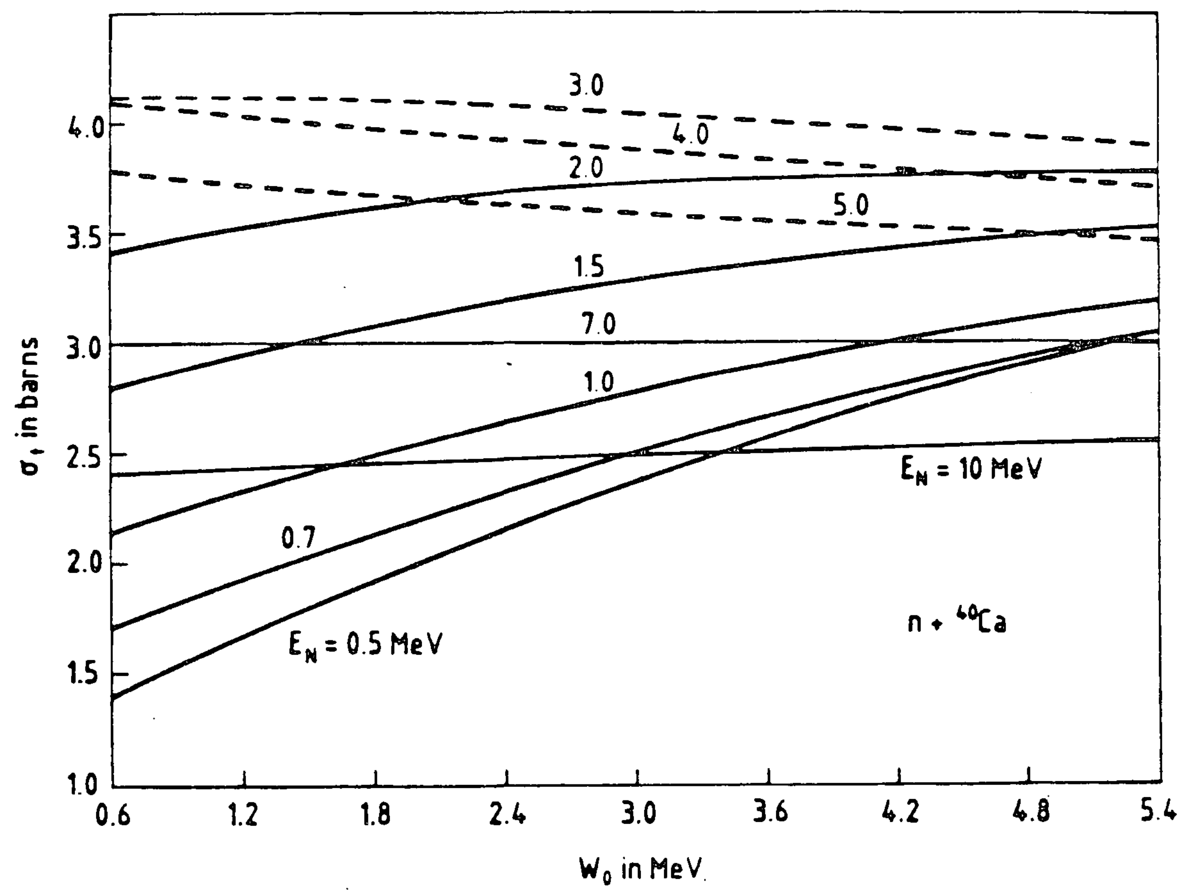

Fig.16 Total cross section for the interaction of neutrons with ^{40}Ca as a function of the constant term W_0 of the imaginary potential depth for several energies.

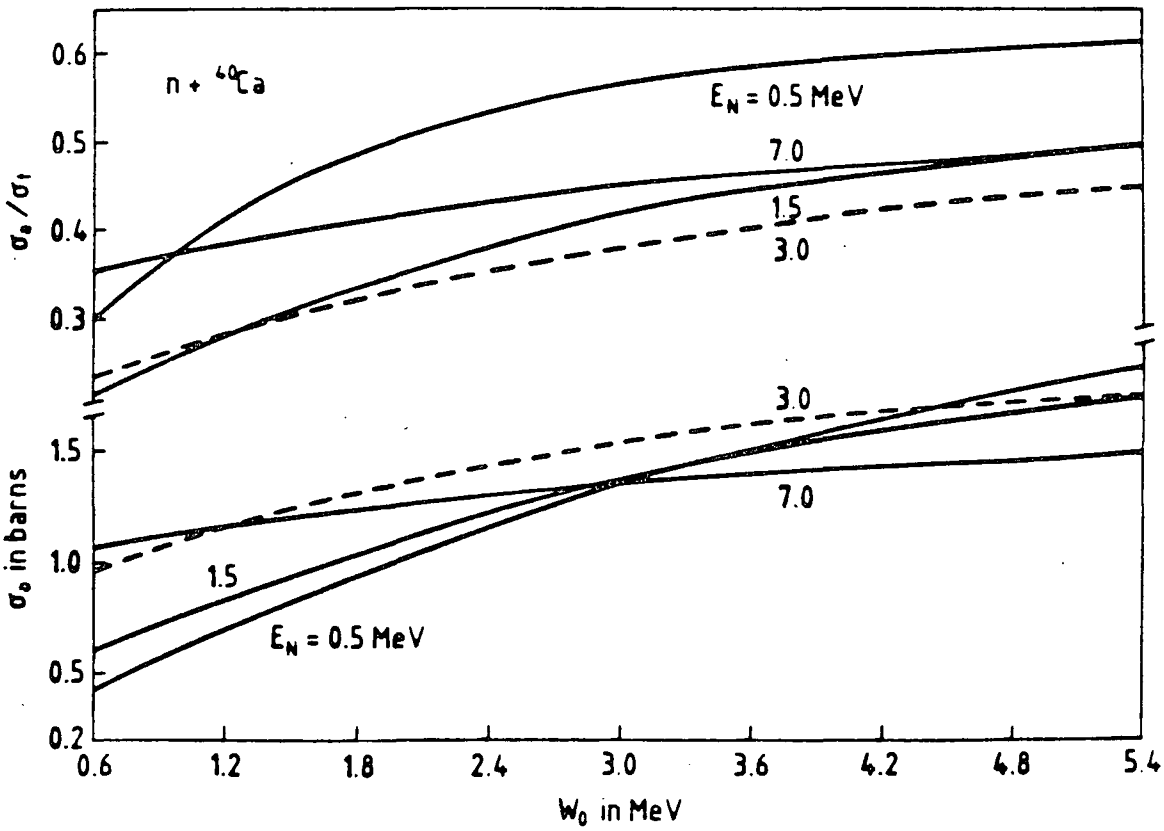

Fig.17 Absorption cross section and σ_a/σ_t for the interaction of neutrons with ^{40}Ca as a function of the constant term W_0 of the imaginary potential depth for several energies.

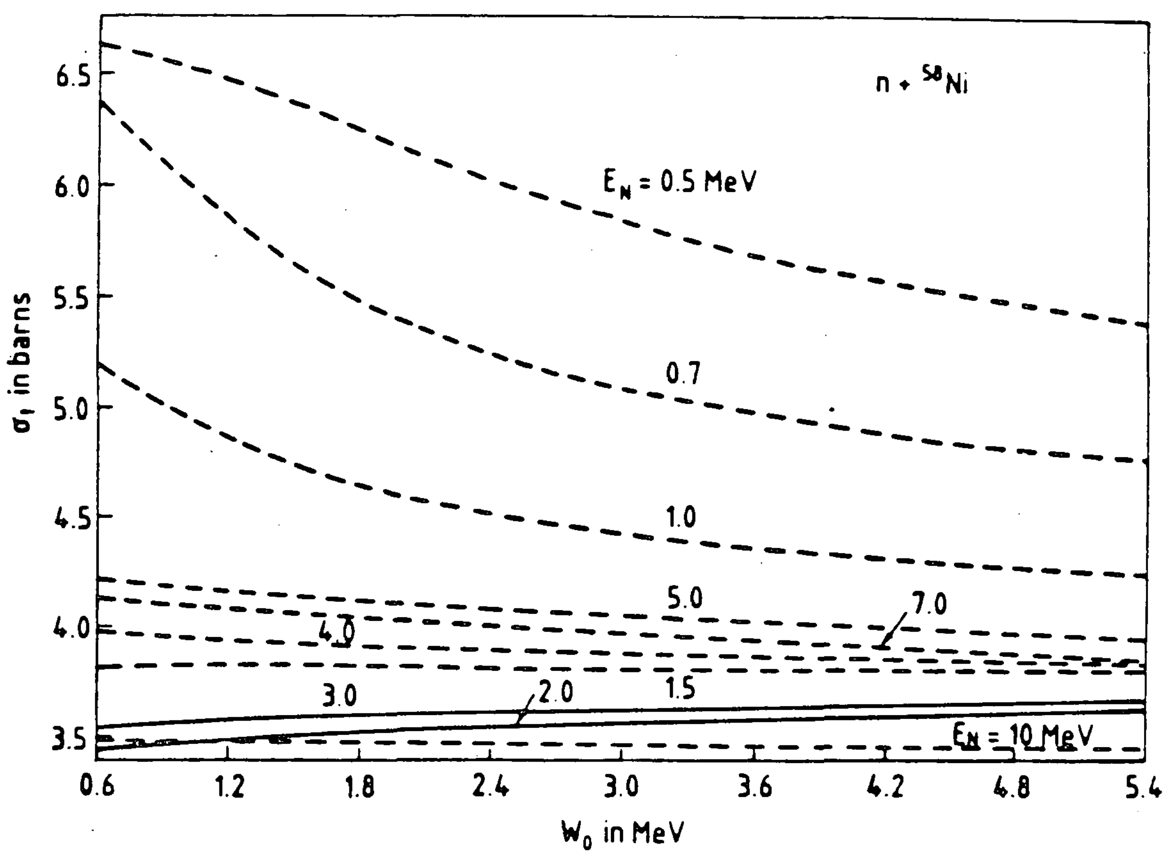

Fig.18 Total cross section for the interaction of neutrons with ^{58}Ni as a function of the constant term W_0 of the imaginary potential depth for several energies.

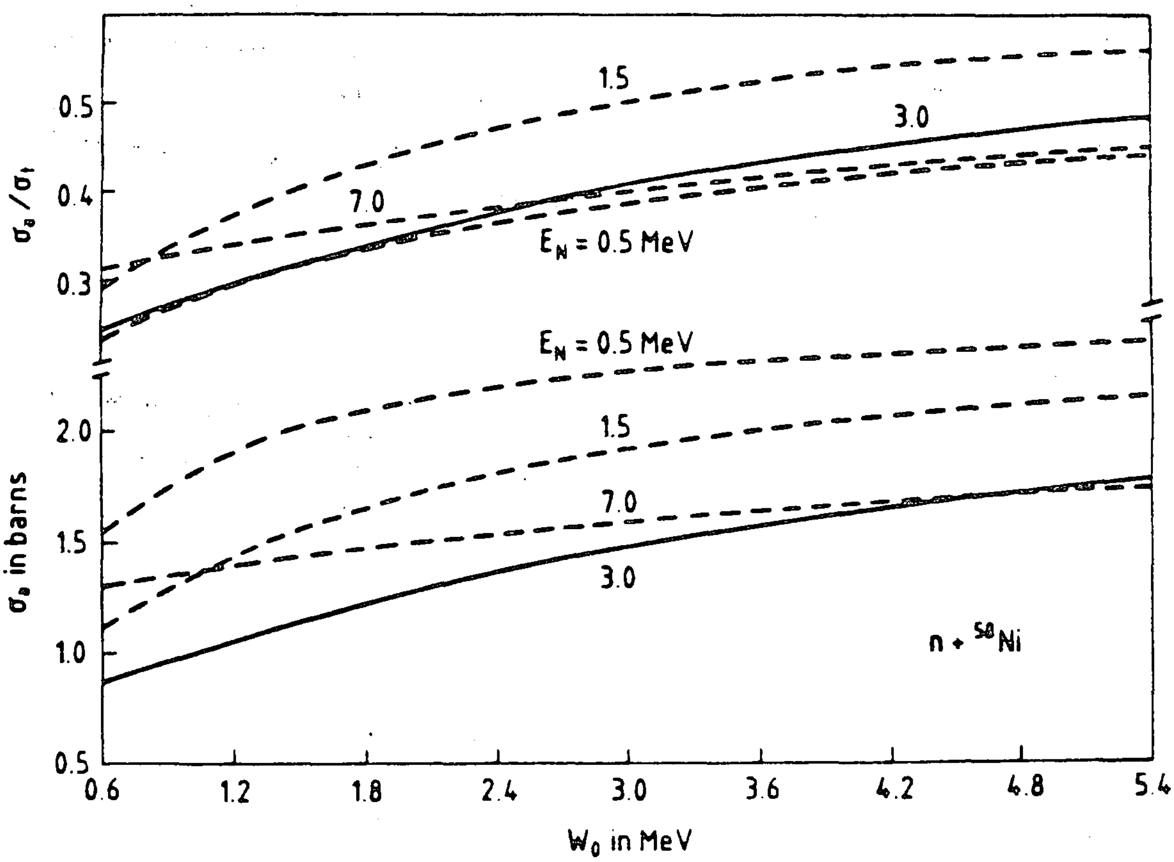

Fig.19 Absorption cross section and σ_a/σ_t for the interaction of neutrons with ^{40}Ca as a function of the constant term W_0 of the imaginary potential depth for several energies.

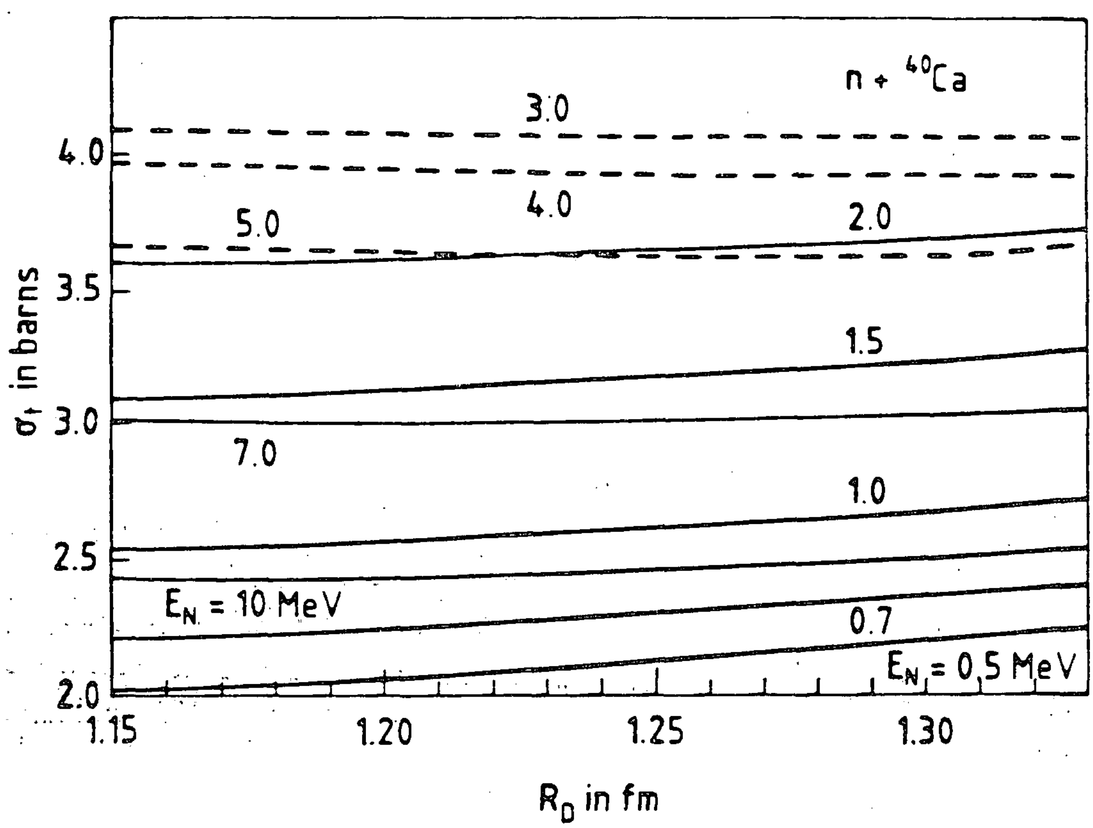

Fig.20 Total cross section for the interaction of neutrons with ^{40}Ca as a function of the radius parameter r_D of the imaginary potential for several energies.

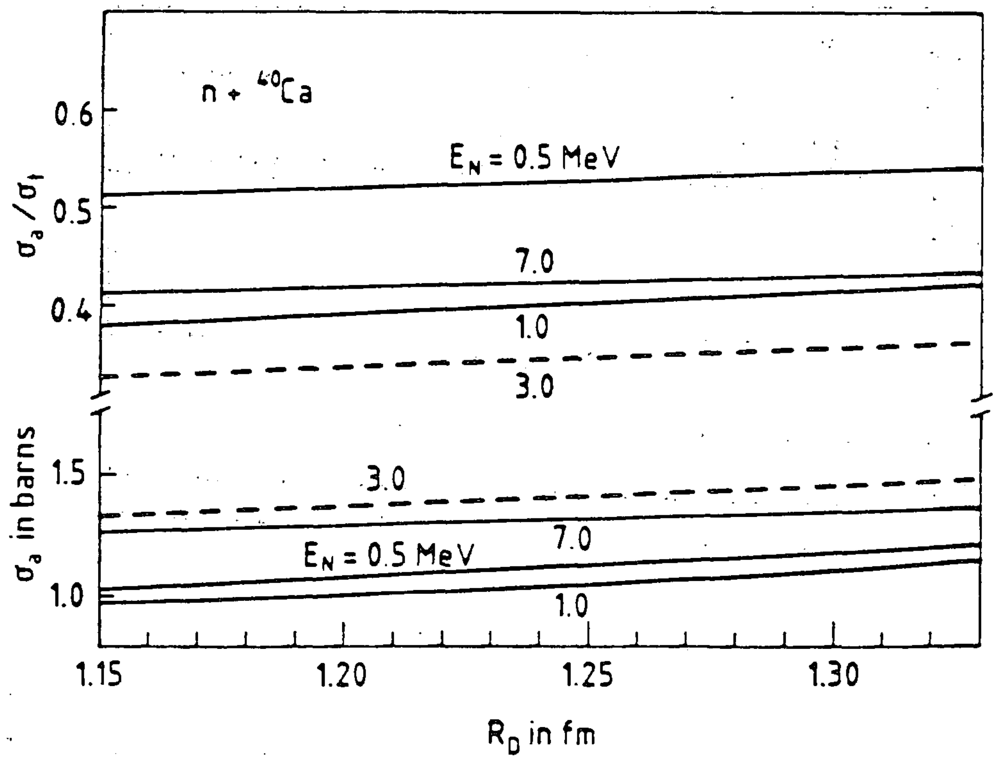

Fig.21 Absorption cross section and σ_a/σ_t for the interaction of neutrons with ^{40}Ca as a function of the radius parameter r_D of the imaginary potential for several energies.

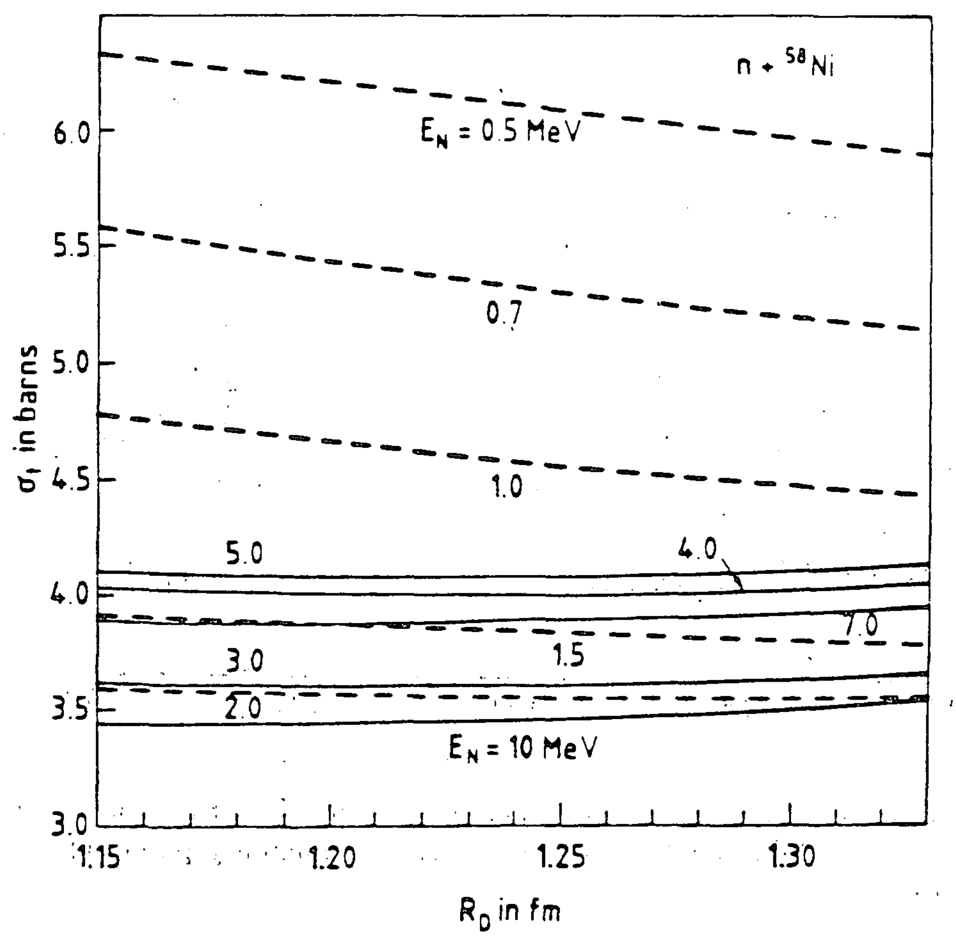

Fig.22 Total cross section for the interaction of neutrons with ^{58}Ni as a function of the radius parameter r_D of the imaginary potential for several energies.

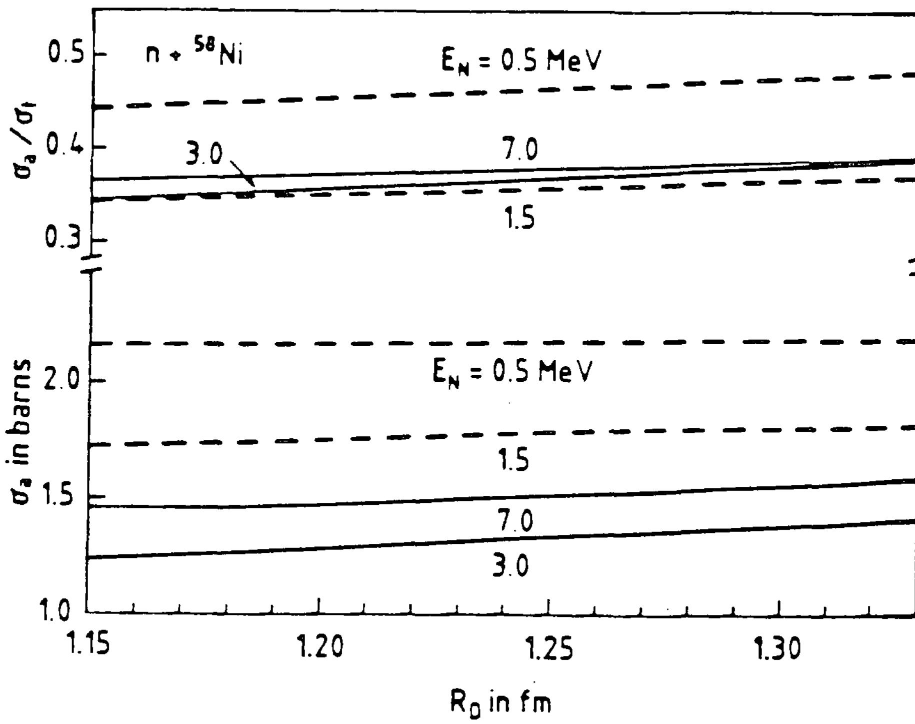

Fig.23 Absorption cross section and σ_a/σ_t for the interaction of neutrons with ^{58}Ca as a function of the radius parameter r_D of the imaginary potential for several energies.

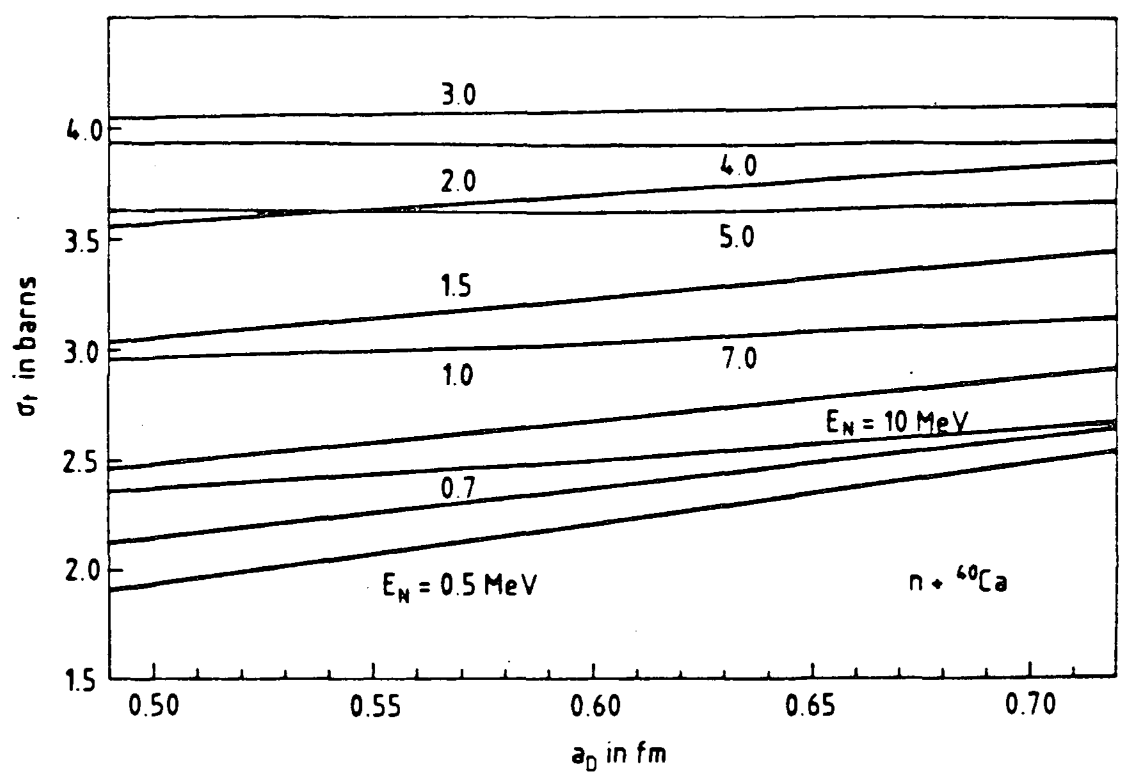

Fig.24 Total cross section for the interaction of neutrons with ^{40}Ca as a function of the surface diffuseness parameter a_D of the imaginary potential for several energies.

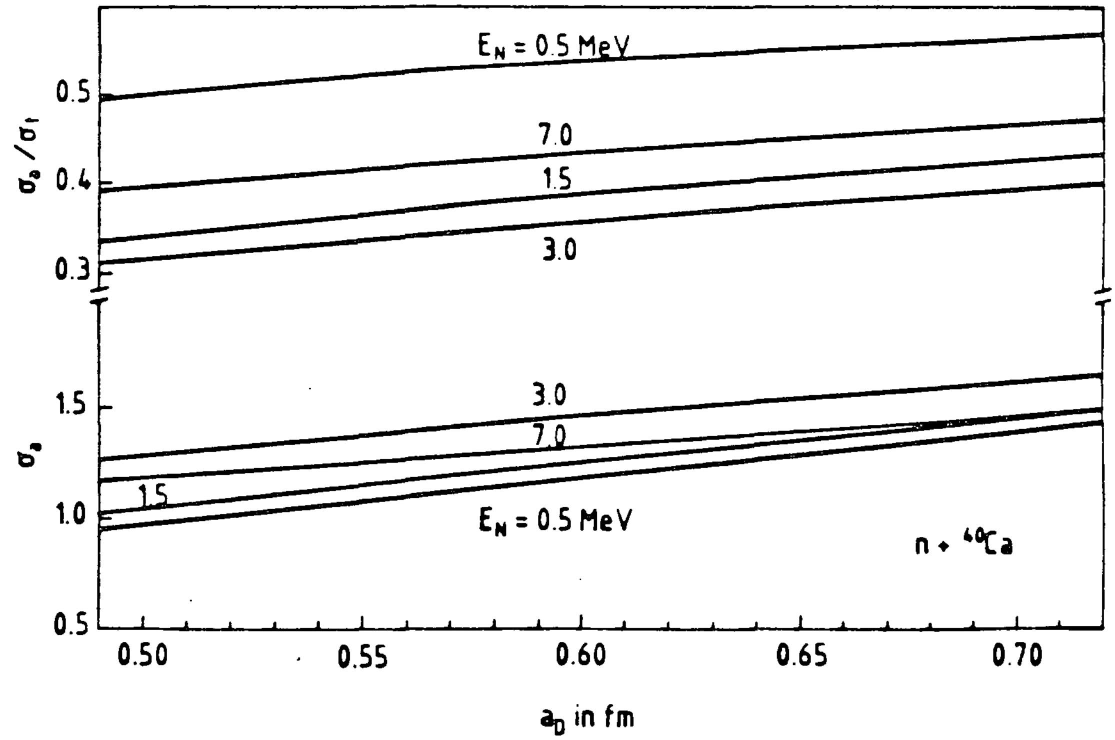

Fig.25 Absorption cross section and σ_a/σ_t for the interaction of neutrons with ^{40}Ca as a function of the surface diffuseness parameter a_D of the imaginary potential for several energies.

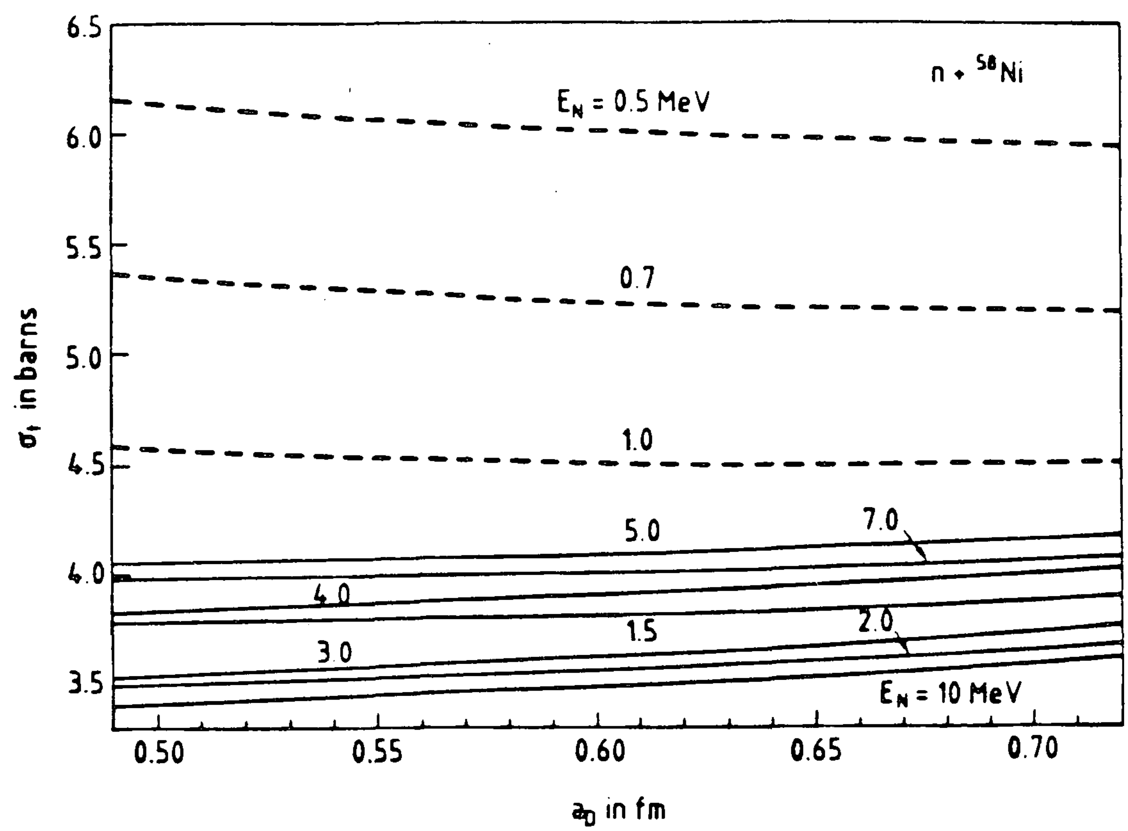

Fig.26 Total cross section for the interaction of neutrons with ^{58}Ni as a function of the surface diffuseness parameter a_D of the imaginary potential for several energies.

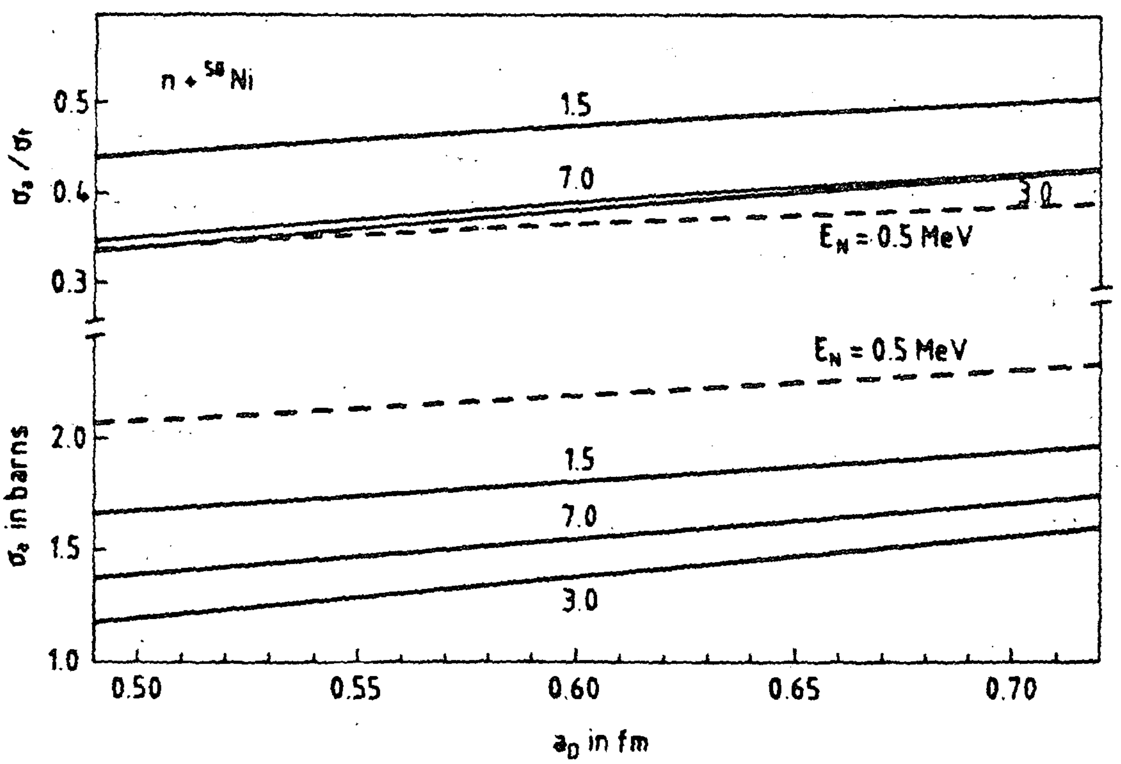

Fig.27 Absorption cross section and σ_a/σ_t for the interaction of neutrons with ^{58}Ca as a function of the surface diffuseness parameter a_D of the imaginary potential for several energies.